

echo echo-planar imaging (GE-EPI) was used; field of view (FOV) =  $128 \times 128$  mm, repetition time (TR) = 750 ms, echo time (TE) = 18.4 or 20 ms, flip angle = 64 degrees, matrix =  $64 \times 64$ , slice thickness = 2 mm, interslice gap = 0.5 mm, 9 transverse slices]. Image distortions from the susceptibility artifact were negligible, and the EPI-images overlapped faithfully with the reference images (Fig. 2D). Functional images were first realigned, spatially normalized to a template with interpolation to a  $1 \times 1 \times 1$  mm space and then smoothed with a Gaussian kernel [full width at half maximum (FWHM) 4 mm]. The template was made from 3D-structural images of one monkey's whole brain (24) and was arranged in bicommissural space (16). The origin was placed at the anterior commissure. In separate sessions, high-resolution 3D-anatomical scans of monkeys were obtained using both the 3D-gradient-echo sequence (voxel =  $1 \times 1 \times 1$  mm) and the 3D-MDEFT (modified driven equilibrium Fourier transform) sequence (voxel =  $0.5 \times 0.5 \times 0.5$  mm).

24. J. Ashburner, K. J. Friston, *NeuroImage* 6, 209 (1997).

25. Data were analyzed using the general linear model for event-related designs in SPM99 (<http://www.fil.ion.ucl.ac.uk/spm/>). Transient events during dimensional changes were coded using the hemodynamic response function implemented in SPM 99. The onset of each hemodynamic response function was aligned at the onsets of the incorrect feedback stimuli just before the completion of each shifting (Fig. 1C). Error trials were coded independently. In monkey experiments, statistical results are based on a single-voxel threshold of  $P < 0.05$ , corrected for multiple comparisons across the brain volume examined. In human experiments, a random effect model was used for estimating the data, and we assessed statistical significance at the threshold of 19 or more contiguous significant voxels above the  $P < 0.001$  (uncorrected) (29).

26. Supplementary materials of Tables 1 and 2 are available on Science Online at [www.sciencemag.org/cgi/content/full/295/5559/1532/DC1](http://www.sciencemag.org/cgi/content/full/295/5559/1532/DC1)

27. K. J. Friston, A. P. Holmes, K. J. Worsley, *NeuroImage* 10, 1 (1999).

28. In human experiments, informed consent was obtained from ten healthy right-handed subjects. They were scanned using experimental procedures approved by the institutional review board of the University of Tokyo School of Medicine. Functional MRI scans were performed on the same 1.5 T scanner as in the monkey experiments with single-shot GE-EPI (FOV =  $256 \times 256$  mm, TR = 4 s, TE = 50 ms, flip angle = 90 degrees, matrix =  $64 \times 64$ , slice thickness = 4 mm, 28 transverse slices). Functional images were realigned, spatially normalized to a template with interpolation to a  $2 \times 2 \times 2$  mm space, and smoothed with a Gaussian kernel (FWHM 8 mm).

29. S. Konishi, D. I. Donaldson, R. L. Buckner, *NeuroImage* 13, 364 (2001).

30. K. F. Berman et al., *Neuropsychologia* 33, 1027 (1995).

31. Y. Nagahama et al., *Brain* 119, 1667 (1996).

32. S. Konishi et al., *Nature Neurosci.* 1, 80 (1998).

33. O. Monchi, M. Petrides, V. Petre, K. Worsley, A. Dagher, *J. Neurosci.* 21, 7733 (2001).

34. A. E. Walker, *J. Comp. Neurol.* 73, 59 (1940).

35. K. Brodmann, in *Handbuch der Neurologie*, M. Lewandowsky, Ed. (Springer-Verlag, Berlin, 1910), vol. 1, pp. 206–307.

36. C. J. Bruce, M. E. Goldberg, M. C. Bushnell, G. B. Stanton, *J. Neurophysiol.* 54, 714 (1985).

37. T. Paus, *Neuropsychologia* 34, 475 (1996).

38. I. Hasegawa, T. Fukushima, T. Ihara, Y. Miyashita, *Science* 281, 814 (1998).

39. Surface-based activation displays were constructed using the SureFit software (<http://stp.wustl.edu/>) (12).

40. We thank I. Hasegawa, M. Morita, M. Koyama, and M. Ohbayashi for their help and I. Kanazawa for his encouragement. This work was supported by a Grant-in-Aid for Specially Promoted Research (07102006) from the Ministry of Education, Culture, Sports, Science and Technology (MEXT) of Japan.

1 November 2001; accepted 15 January 2002

## Retrograde Support of Neuronal Survival Without Retrograde Transport of Nerve Growth Factor

Bronwyn L. MacLinnis and Robert B. Campenot\*

Application of nerve growth factor (NGF) covalently cross-linked to beads increased the phosphorylation of TrkA and Akt, but not of mitogen-activated protein kinase, in cultured rat sympathetic neurons. NGF beads or iodine-125-labeled NGF beads supplied to distal axons resulted in the survival of over 80% of the neurons for 30 hours, with little or no retrograde transport of iodine-125-labeled NGF; whereas application of free iodine-125-labeled NGF (0.5 nanograms per milliliter) produced 20-fold more retrograde transport, but only 29% of the neurons survived. Thus, in contrast to widely accepted theory, a neuronal survival signal can reach the cell bodies unaccompanied by the NGF that initiated it.

The literatures of neuronal development, neurotrauma, degenerative neurological disease, and neuronal regeneration are pervaded by the concept that the survival and function of neurons depend on retrograde transport of neurotrophic factors released from the target cells that they innervate. This idea began with the discovery that nerve growth factor (NGF) is retrogradely transported from axon terminals to neuronal cell bodies (1–7). The current theory, that NGF complexed with its receptor, TrkA, is endocytosed, trafficked to signaling endosomes (8, 9), and retrogradely

transported to the cell bodies, has been supported by results of studies with compartmented cultures (10–14). However, Senger and Campenot (15) observed retrograde phosphorylation of TrkA and other proteins occurring 1 to 15 min after NGF application, preceding the arrival of detectable  $^{125}\text{I}$ -NGF by at least 30 min.

We examined this issue using NGF covalently cross-linked to beads to prevent internalization (16). Mass cultures of rat sympathetic neurons (17) that had been deprived of NGF (18) displayed a similar level of phosphorylation of TrkA (19) after 1 hour of application of free NGF (50 ng/ml) or NGF beads (50  $\mu\text{l/ml}$ ) (Fig. 1A). NGF and NGF beads also induced the phosphorylation of Akt (Fig. 1B), the latter suggesting that phosphorylated TrkA (pTrkA) at the plasma

membrane can activate phosphatidylinositol 3-kinase (PI 3-kinase). In contrast, little mitogen-activated protein kinase (MAPK) phosphorylation was observed in response to NGF beads (Fig. 1B), suggesting that internalization of pTrkA is necessary for the activation of MAPK. This result is consistent with reports that the blockage of endocytosis of TrkA, by means of pharmacological inhibitors or dominant-negative dynamin, inhibits NGF-induced MAPK phosphorylation in dorsal root ganglion neurons (20) and PC12 cells (20–22). Thus, the lack of NGF-induced MAPK phosphorylation that we observed suggests that neither NGF nor TrkA is internalized when NGF is presented in bead-linked form.

To determine whether NGF beads can produce retrograde signals, distal axons of sympathetic neurons in NGF-deprived compartmented cultures (17, 18) received different NGF treatments for 30 hours, and neuronal survival was assayed (23). Treatment with NGF beads resulted in 81% neuronal survival (Fig. 2, A and B), which approaches the survival in cultures given free NGF (50 ng/ml) (95%) and is almost four times the survival of cultures given no NGF (22%). Control beads to which NGF was not covalently cross-linked did not support survival (Fig. 2B). Retrograde survival could conceivably have been achieved by the release of NGF from the beads into the culture medium, followed by internalization and retrograde transport. However, supernatant media from NGF beads that had supported 30 hours of retrograde survival of one set of cultures (Fig. 2C, solid bars) failed to support survival of a second set of cultures (Fig. 2C, hatched bars), whereas free NGF from the first set again supported the survival of a second set. Supernatant media from NGF beads that were preincubated

Department of Cell Biology, 6–14 Medical Sciences Building, University of Alberta, Edmonton, Alberta, Canada, T6G 2H7.

\*To whom correspondence should be addressed. E-mail: bob.campenot@ualberta.ca

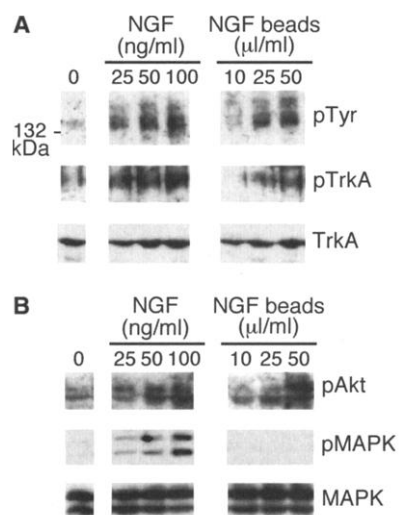
for 30 hours without neurons present also failed to support neuronal survival (Fig. 2C, open bars), ruling out the possibility that NGF released from the beads may have been depleted from the medium by retrograde transport.

To directly assess possible retrograde transport of NGF from beads, we compared the retrograde transport of <sup>125</sup>I originating from a range of concentrations of free <sup>125</sup>I-NGF with transport from bead-linked <sup>125</sup>I-NGF (50 μl/ml) (24). Iodination did not affect the ability of free NGF or bead-linked NGF to induce TrkA phosphorylation (Fig. 3A). Because 90% of the <sup>125</sup>I transported to the cell bodies over 30 hours had been released into the center compartment medium (7, 15), we assessed retrograde transport by gamma counts of the center compartment medium and assayed the survival of the same neurons by Hoechst staining (23). Provision of <sup>125</sup>I-NGF beads to distal axons supported the survival, on average, of 84% of the neurons, whereas retrograde transport by these neurons was barely detected at 0.57 pg of NGF per culture (Fig. 3B). Cultures given 50 ng/ml of free <sup>125</sup>I-NGF displayed 96% survival associated with transport of over 1000-fold more NGF (657 pg per culture), and even cultures given 0.5 ng/ml of free <sup>125</sup>I-NGF,

which displayed only 29% survival, transported over 20-fold more NGF (12 pg per culture). The high-performance liquid chromatography (HPLC)-purified <sup>125</sup>I-NGF was more than 97% pure iodinated species (24). Therefore, the possibility that unlabeled NGF was present, selectively released from the beads, and retrogradely transported, resulting in neuronal survival, can be ruled out. Thus, by providing NGF in bead-linked form, we have supported neuronal survival while virtually eliminating the retrograde transport of NGF observed when survival is supported by free NGF.

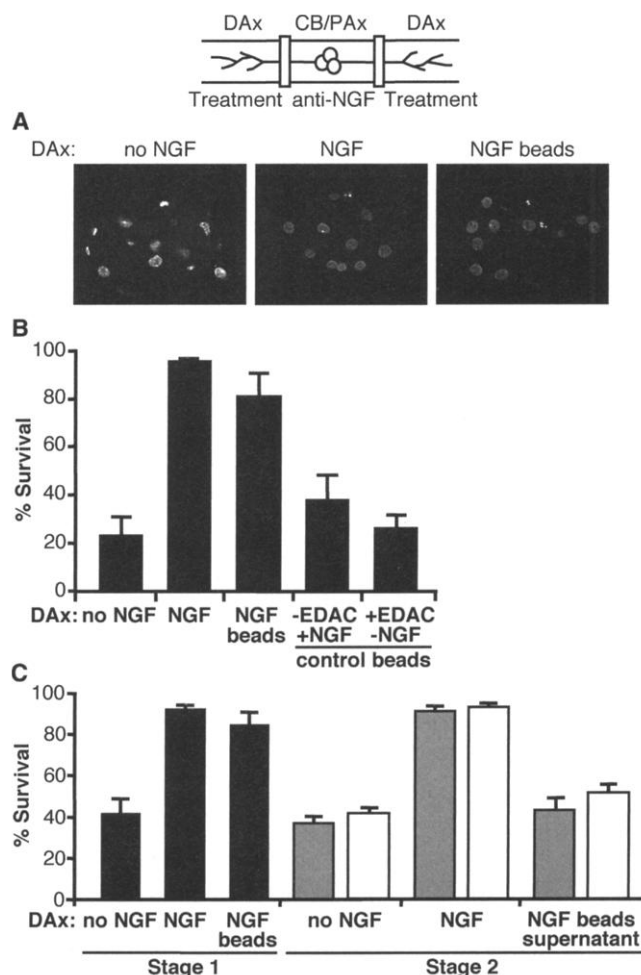
Because NGF beads activate Akt, presumably via PI 3-kinase, we investigated whether blockage of PI 3-kinase activity with 50 μM LY294002 (LY) (25) could block retrograde survival signaling from NGF and NGF beads. In cultures given NGF in all compartments, LY applied to

distal axons blocked NGF-induced Akt phosphorylation in the distal axons without effect on Akt phosphorylation in the cell bodies/proximal axons and vice versa as previously shown (14), indicating that LY can be used to locally block PI 3-kinase. NGF-deprived cultures displayed 40% survival, whereas provision of free NGF to distal axons increased survival to 99%, giving a free NGF-induced survival component of 59% of the population of neurons (Fig. 4). When LY was applied to cell bodies/proximal axons, the NGF-induced survival component was only 6%; but when LY was applied to distal axons, little inhibition was observed, with 47% NGF-induced survival. These results are consistent with a previous report (14). Provision of NGF beads to distal axons resulted in total survival of 79% of the neurons, giving an NGF bead-induced survival component of



**Fig. 1.** Phosphorylation of TrkA, Akt, and MAPK in response to NGF and NGF beads. Mass cultures (17) were deprived of NGF (18) and incubated for 1 hour with medium lacking NGF, medium containing free NGF, or NGF beads at the concentrations indicated. Cell extracts were analyzed by immunoblot (19). All lanes are from the same PVDF membrane. Blots are representative of three experiments with similar results. (A) Proteins >100 kD were probed with antibody to phosphotyrosine (pTyr), stripped, reprobbed with antibody to phosphoTrkA Y490 (pTrkA), stripped, and reprobbed with antibody to TrkA (TrkA). (B) Proteins <100 kD were probed with antibody to phosphoAkt (pAkt), reprobbed with antibody to phosphoMAPK (pMAPK), stripped, and reprobbed with antibody to p44 MAPK (MAPK).

**Fig. 2.** NGF beads support retrograde survival of sympathetic neurons. Compartmented cultures were deprived of NGF (18), and distal axons (Dax) were given the indicated treatments for 30 hours while cell bodies/proximal axons (CB/Pax) were exposed to antibody to NGF. Then the nuclei were stained with Hoechst DNA stain to assess neuronal survival (23). (A) Confocal micrographs of representative neurons treated with no NGF, free NGF (50 ng/ml), and NGF beads (50 μl/ml). (B) A minimum of 1000 neurons were categorized per treatment group as surviving (diffusely labeled DNA) or dying/dead (condensed fragmented DNA or unlabeled). The percentage of live neurons in each treatment group (±SEM, n = 3 cultures) is plotted. The two bead control groups were given NGF beads (50 μl/ml) prepared without EDAC cross-linking or beads (50 μl/ml) cross-linked without NGF present (16). Results are representative of three experiments. (C) Stage 1: Distal axons of NGF-deprived cultures were treated for 30 hours with no NGF, free NGF, or NGF beads as in (B), and neuronal survival was determined (black bars). Concurrently, aliquots of these media were incubated in dishes under culturing conditions, but without neurons present. Stage 2: media from the distal axons of all groups were collected at the end of stage 1, beads were removed from the NGF-bead medium by centrifugation, and these media were used to treat distal axons of NGF-deprived neurons for 30 hours in a second set of cultures (gray bars). The supernatants from aliquots incubated without neurons during stage 1 were also tested (white bars). Data are combined from two experiments (n = 6 cultures ± SEM).



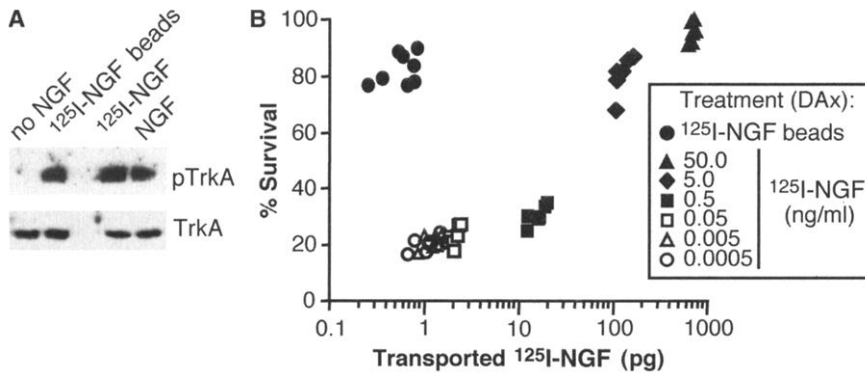


**Fig. 3.** Relationship between NGF retrograde transport and neuronal survival for free NGF and NGF beads. **(A)** The ability of <sup>125</sup>I-NGF beads (50 μl/ml), <sup>125</sup>I-NGF (50 ng/ml), and unlabeled NGF (50 ng/ml) to induce tyrosine phosphorylation of TrkA in NGF-deprived mass cultures was tested as described in Fig. 1. **(B)** NGF-deprived neurons in compartmented cultures (18) were provided with the indicated concentrations of free <sup>125</sup>I-NGF or <sup>125</sup>I-NGF beads (50 μl/ml) applied to distal axons (DAX) for 30 hours. Then medium bathing the cell bodies/proximal axons was collected, and transported radioactivity was determined (24). Neuronal survival was determined in the same cultures by examination of Hoechst-stained nuclei of at least 250 neurons per culture (23). The percent survival is plotted against transported <sup>125</sup>I-NGF for each individual culture (three or four per group) from three experiments.

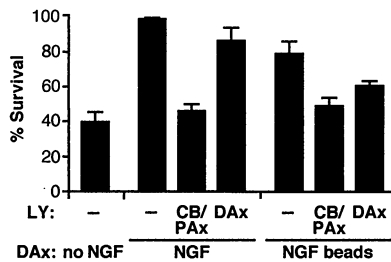


**Fig. 4.** Effects of LY294002 (LY) on retrograde survival supported by NGF and NGF beads. Compartmented cultures were deprived of NGF (18), and distal axons were given no NGF, NGF (50 ng/ml), or NGF beads (50 μl/ml) for 30 hours. Concurrently, the cell bodies/proximal axons (CB/PAX) or distal axons (DAX) were given 50 μM LY as indicated. Then the neuronal survival of at least 250 neurons per culture was assayed as in Fig. 2 (23). The percentage of live neurons in two replicate experiments is plotted (±SEM, n = 6 cultures). LY from Sigma was made as a 50 mM stock in dimethylsulfoxide. All compartments not given LY received equivalent dimethylsulfoxide, which was 0.1% of culture medium.

39%. Application of LY to cell bodies/proximal axons reduced this to 8%, similar to the inhibition of free NGF-induced survival. However, application of LY to the distal axons inhibited the survival induced by NGF beads by about half, to 20% (paired sample *t* test, *P* < 0.002). This suggests that PI 3-kinase activity in the distal axons may be more important in generating retrograde signals from NGF beads, possibly because this pathway can be activated without internalization, whereas other survival pathways may require internalization.

What possible mechanisms of retrograde signaling are consistent with our results? Be-

cause 50% of sympathetic neurons commit to apoptosis after 18 hours of NGF deprivation (26), and the survival signal must travel at least 1.5 mm to reach the cell bodies, diffusion of proteins 15 kD or larger is ruled out (27). Another possibility is that phosphorylation of TrkA bound to NGF beads propagated to neighboring unbound TrkA at the plasma membrane, as observed for EGF activation of ErbB1 receptors (28). Serial TrkA phosphorylation could conceivably propagate along the proximal axons to the cell bodies, as suggested by Senger and Campenot (15). Also, NGF beads could induce the internalization and retrograde transport of pTrkA in the absence of the NGF that initiated it, although it is unclear how TrkA would remain phosphorylated. Transport of activated downstream signaling molecules (29) and ionic propagation mechanisms involving release of calcium into the cytosol (15) have also been suggested. Our results raise the possibility that retrograde transport of NGF may not be required for any mechanism of retrograde signaling, but other studies present evidence that neurotrophin transport is required (10–14). Although we find this evidence inconclusive (30), different mechanisms of retrograde signaling are not mutually exclusive. Perhaps propagated signals operate early in neuronal development and/or during axonal regeneration after injury. At these times, axon terminals consist of a few growth cones, and the neurotrophic factors they encounter may have to produce amplified signals to be effective. There are many speculative scenarios, but clearly the assumption of over 25 years that retrograde transport of NGF (and all other neurotrophic factors) is the only way that retrograde signals can reach the cell bodies needs continued reexamination.

References and Notes

1. I. A. Hendry, K. Stockel, H. Thoenen, L. L. Iversen, *Brain Res.* **68**, 103 (1974).
2. K. Stockel, M. Schwab, H. Thoenen, *Brain Res.* **99**, 1 (1975).
3. P. Claude, E. Hawrot, D. A. Dunis, R. B. Campenot, *J. Neurosci.* **2**, 431 (1982).
4. S. Korsching, H. Thoenen, *Neurosci. Lett.* **39**, 1 (1983).
5. M. A. Palmatier, B. K. Hartman, E. M. Johnson Jr., *J. Neurosci.* **4**, 751 (1984).
6. D. R. Ure, R. B. Campenot, *Dev. Biol.* **162**, 339 (1994).
7. ———, *J. Neurosci.* **17**, 1282 (1997).
8. M. L. Grimes *et al.*, *J. Neurosci.* **16**, 7950 (1996).
9. M. L. Grimes, E. Beattie, W. C. Mobley, *Proc. Natl. Acad. Sci. U.S.A.* **94**, 9909 (1997).
10. F. L. Watson *et al.*, *J. Neurosci.* **19**, 7889 (1999).
11. A. Riccio, B. A. Pierchala, C. L. Ciarallo, D. D. Ginty, *Science* **277**, 1097 (1997).
12. B. A. Tsui-Pierchala, D. D. Ginty, *J. Neurosci.* **19**, 8207 (1999).
13. F. L. Watson *et al.*, *Nature Neurosci.* **4**, 4 (2001).
14. R. Kuruvilla, H. Ye, D. D. Ginty, *Neuron* **27**, 499 (2000).
15. D. L. Senger, R. B. Campenot, *J. Cell Biol.* **138**, 411 (1997).
16. NGF was covalently cross-linked using EDAC [1-ethyl-3-(3-dimethylaminopropyl) carbodiimide, hydrochloride] to 1-μm-diameter FluoSperes amine-modified microspheres (Molecular Probes, Eugene, OR) (17). Beads were resuspended in phosphate-buffered saline (PBS) at a final concentration of 0.1% beads per volume to avoid agglomeration. With the exception of <sup>125</sup>I-NGF beads, which were used within 36 hours, NGF beads were used for experiments immediately after preparation. All treatment groups not given beads received an equivalent volume of PBS. Two preparations of control beads were made according to the same protocol, but either EDAC or NGF was omitted. Neither induced TrkA phosphorylation when tested in mass cultures.
17. Dissociated superior cervical ganglion neurons (31, 32) from newborn Sprague-Dawley rats (University of Alberta Health Sciences Lab Animal Services) were mass cultured in L15CO<sub>2</sub> medium with 2.5% rat serum and NGF (50 ng/ml) in 24-well Linbro tissue culture dishes (ICN Biomedicals, Aurora, OH) at one ganglion per two wells. For compartmented cultures (31, 32), the neurons (0.25 ganglion per culture) were plated into the center compartments of Camp 10 dishes (Tyler Research, Edmonton, Alberta, Canada) in L15CO<sub>2</sub> medium with 2.5% rat serum and 20 ng of NGF/ml. Left and right distal compartments were supplied with L15CO<sub>2</sub> medium with NGF (100 ng/ml). From day 7, center compartments were no longer provided with NGF. Identically maintained sister cultures, 7 to 10 days old, were used in each experiment.
18. Neurons in mass cultures were deprived of NGF by exposure for 6 hours to medium containing no NGF and sheep anti-NGF (24 nM; Cedarlane Laboratories Limited, Hornby, Ontario, Canada). They were rinsed once with culture medium without additives and incubated for 1 hour with medium lacking NGF to remove the antibodies. Neurons in compartmented cultures were deprived of NGF by incubation with medium containing antibodies to NGF in all compartments for 3 hours. Antibodies to NGF were removed from the distal axon compartments by washing twice with unsupplemented culture medium over a 30-min period. Antibodies to NGF were supplied to the cell bodies/proximal axons for the full duration of all survival experiments.
19. For immunoblotting, two mass culture wells per treatment group were rinsed with ice-cold tris-buffered saline containing 1 mM sodium orthovanadate and 10 mM sodium fluoride, lysed directly into sodium dodecyl sulfate (SDS) sample buffer, boiled for 5 min, resolved on 8% SDS gels, and wet transferred (Hoffer Scientific Instruments, San Francisco, CA) to Immobilon-P polyvinylidene difluoride (PVDF) membrane (Millipore Corp., Bedford, MA). We immunoblotted with the following antibodies at the indicated dilutions: monoclonal antibody (mAb) to phosphotyrosine (clone 4G10) (1:2000) (Upstate Biotechnology, Lake Placid, NY), polyclonal antibody (pAb) to phosphoTrkA (Y490) (1:1000), mAb

to phospho-p44/p42 MAPK (Thr<sup>202</sup>/Tyr<sup>204</sup>) (1:5000), and pAb to phosphoAkt (Ser<sup>473</sup>) (1:1000) (Cell Signaling Technology, Beverly, MA). Gel loading of total TrkA and MAPK was determined by immunoblotting with pAb to TrkA (C-14) (1:2000) and pAb to p44 MAPK (C-16) (1:2000) (Santa Cruz Biotechnology, Santa Cruz, CA), which reacts with both p44 and p42 MAPK. Immunoreactivity was detected by enhanced chemiluminescence (SuperSignal West Dura Substrate, Pierce, Rockford, IL). Blots were stripped with Restore Western Blot Stripping Buffer (Pierce) according to the manufacturer's directions.

20. R. D. York *et al.*, *Mol. Cell. Biol.* **20**, 8069 (2000).

21. Y. Zhang, D. B. Moheban, B. R. Conway, A. Bhattacharyya, R. A. Segal, *J. Neurosci.* **20**, 5671 (2000).

22. S. Rakhit, S. Pyne, N. J. Pyne, *Mol. Pharmacol.* **60**, 63 (2001).

23. Neuronal survival was assessed by Hoechst staining of DNA. Cultures were fixed with 4% paraformaldehyde at room temperature for 20 min and incubated in Hoechst 33258 dye (50 mM in PBS; Molecular Probes) for 30 min. Confocal images were obtained with a Zeiss LSM 510 laser scanning microscope (Carl Zeiss, Jena, Germany). Stained nuclei were quantified

using a Nikon Eclipse TE300 inverted fluorescence microscope (Nikon, Tokyo, Japan).

24. Mouse NGF (2.5S, grade II; Alomone Labs, Jerusalem, Israel) was commercially conjugated to <sup>125</sup>I by ICN Radiochemicals (Irvine, CA) using the lactoperoxidase/H<sub>2</sub>O<sub>2</sub> method without carrier protein. Unconjugated NGF and <sup>125</sup>I were removed by HPLC, yielding greater than 97% purity of <sup>125</sup>I-NGF with a specific activity at the time of the experiments of 38.2 mCi/mg. Transported <sup>125</sup>I-NGF was measured by  $\gamma$ -counting the medium bathing the cell bodies/proximal axons (7, 15). Control cultures for nonspecific transport were given medium containing <sup>125</sup>I-NGF plus 100 $\times$  excess of unlabeled NGF; and mean nonspecific transport, which was less than 5% of transport obtained with free <sup>125</sup>I-NGF (50 ng/ml), was subtracted from mean transport of each group. The <sup>125</sup>I-NGF and <sup>125</sup>I-NGF beads within an experiment were from the same preparation.

25. C. J. Vlahos, W. F. Matter, K. Y. Hui, R. F. Brown, *J. Biol. Chem.* **269**, 5241 (1994).

26. T. L. Deckwerth, E. M. Johnson Jr., *J. Cell Biol.* **123**, 1207 (1993).

27. S. Popov, M. M. Poo, *J. Neurosci.* **12**, 77 (1992).

28. P. J. Verwee, F. S. Wouters, A. R. Reynolds, P. I. Bastiaens, *Science* **290**, 1567 (2000).

29. I. A. Hendry, M. F. Crouch, *Neurosci. Lett.* **133**, 29 (1991).

30. K. E. Neet, R. B. Campenot, *Cell. Mol. Life Sci.* **58**, 1021 (2001).

31. R. B. Campenot, in *Cell-Cell Interactions: A Practical Approach*, B. R. Stevenson, W. J. Gallin, D. L. Paul, Eds. (IRL Press, Oxford, 1992), pp. 275–298.

32. R. B. Campenot, G. Martin, in *Protocols for Neural Cell Culture*, S. Federoff, A. Richardson, Eds. (Humana Press, Totowa, NJ, 2001), pp. 49–57.

33. Supported by operating grants from the Canadian Institutes of Health Research and the Canadian Neurotrauma Fund. B.L.M. is supported by a studentship from the Canadian Institutes of Health Research. R.B.C. is a Medical Scientist of the Alberta Heritage Foundation for Medical Research. We thank G. Martin for technical assistance; V. Chlumecky for assistance with confocal microscopy; E. Possé de Chavez for use of the fluorescence microscope; E. Shibuya for many helpful discussions; and E. Possé de Chavez, R. Rachubinski, and Z. Wang for reading the manuscript.

31 July 2001; accepted 3 January 2002

## T Cell Receptor Signaling Precedes Immunological Synapse Formation

Kyeong-Hee Lee,<sup>1</sup> Amy D. Holdorf,<sup>1</sup> Michael L. Dustin,<sup>2</sup> Andrew C. Chan,<sup>3</sup> Paul M. Allen,<sup>1</sup> Andrey S. Shaw<sup>1\*</sup>

The area of contact between a T cell and an antigen-presenting cell (APC) is known as the immunological synapse. Although its exact function is unknown, one model suggests that it allows for T cell receptor (TCR) clustering and for sustained signaling in T cells for many hours. Here we demonstrate that TCR-mediated tyrosine kinase signaling in naïve T cells occurred primarily at the periphery of the synapse and was largely abated before mature immunological synapses had formed. These data suggest that many hours of TCR signaling are not required for T cell activation. These observations challenge current ideas about the role of immunological synapses in T cell activation.

The biochemical pathways that are stimulated by TCR engagement are well characterized, but little is known about how T cell interactions with the APC actually initiate signaling by the TCR. The immunological synapse hypothesis proposes that membrane protein reorganization at the T cell–APC contact surface serves to generate a structure, the immunological synapse, which facilitates TCR signaling by concentrating both TCRs and antigenic major histocompatibility complex (MHC)–peptide complexes as well as lipid rafts in the center of the contact [reviewed in (1, 2)]. The stability of this structure can

explain how TCR engagement can be sustained for long periods of time (3).

The immunological synapse was first described as having two discrete zones by using high-resolution immunofluorescence imaging of T cell–APC conjugates (4). The central zone, the c-SMAC, contains the TCR and surface accessory molecules such as CD4, CD2, and CD28 (3). Surrounding the central zone is a second zone, the p-SMAC, which is enriched for the integrin, LFA-1. Real-time imaging with T cells plated on planar membranes shows that synapse formation occurs with TCRs first engaged by MHC peptide in the periphery of the synapse followed by recruitment of such complexes to the center of the synapse. To date, however, the initial engagement of the TCR in the periphery of the contact has not been visualized in immunological synapses formed with APCs (2). We wished, therefore, to determine where TCR–MHC engagement first occurs during authentic synapse formation and to compare it with known T cell signal transduction events.

Freshly isolated naïve T cells were im-

aged to most closely mimic conditions in vivo. We also reasoned that the higher threshold for activation of naïve T cells might result in slower immunological synapse formation. Naïve T cells were purified from AND TCR transgenic mice that recognize a moth cytochrome c peptide (residues 88 to 103) presented by I-E<sup>k</sup> (5). Freshly isolated T and B cell–depleted splenocytes were used as APCs. Conjugate formation was initiated by centrifuging together T cells and APCs, which had been preincubated with antigenic peptide (6). After various times, cells were fixed and then immunostained for TCR and LFA-1 (6). At the earliest time points (2 through 15 min), we noted that the majority of LFA-1 molecules were recruited to the center of the contact area, whereas TCRs were concentrated at the periphery of the synapse (Fig. 1A). Between 15 and 30 min, this pattern reversed, with TCRs now visible in the center of the contact surrounded by an external ring of LFA-1 (Fig. 1A). By 60 min, TCRs in the synapse were not detectable even though LFA-1 was still concentrated in the synapse. Computer reconstructions of the synapse (from serial confocal images along the z axis) confirmed the peripheral localization of the TCR at early time points (15 min), referred to as an immature immunological synapse, and the central localization of the TCR at later time points (30 min), referred to as a mature immunological synapse (Fig. 1B). Immature synapses were also detected with T cell blasts, but synapse maturation occurred much more rapidly (within 1 to 3 min) and the magnitude of TCR down-regulation was much less (7).

To relate the events in the formation of the immature and mature immunological synapse to TCR-mediated signaling, we used phospho-specific antibodies that recognize the activated forms of two key TCR-regulated cytoplasmic tyrosine kinases, Lck and ZAP-70.

<sup>1</sup>Department of Pathology and Immunology, Washington University School of Medicine, 660 South Euclid, Box 8118, Saint Louis, MO 63110, USA. <sup>2</sup>Program in Molecular Pathogenesis, Skirball Institute of Biomolecular Medicine, New York University, 540 First Avenue, New York, NY 10016, USA. <sup>3</sup>Genentech, Department of Immunology, 530 Forbes Boulevard, One DNA Way, South San Francisco, CA 94080, USA.

\*To whom correspondence should be addressed. E-mail: shaw@pathbox.wustl.edu